Reactive and Functional Polymers 213 (2025) 106268

Contents lists available at ScienceDirect

Reactive and Functional Polymers

journal homepage: www.elsevier.com/locate/react

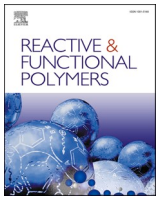

Influence of thermal orientation on the dielectric properties of dendronised poly(2-oxazoline) hybrid membranes

Mark Henning Wolf [a], Jordi Guardià [b], José Antonio Reina [b], Xavier Montané [b], Marta Giamberini [c], Amparo Ribes-Greus [a,*]

[a] Research Institute for Materials Technology, Universitat Politècnica de València, 46022, Valencia, Spain
[b] Department of Analytical Chemistry and Organic Chemistry, Universitat Rovira i Virgili, 43007 Tarragona, Spain
[c] Department of Chemical Engineering, Universitat Rovira i Virgili, 43007 Tarragona, Spain

ARTICLE INFO

Keywords:
Dielectric Thermal Analysis (DETA)
Side-Chain Liquid-Crystalline Polymer (SCLCP)
Poly(2-oxazoline)
Dendrons
Thermal orientation

ABSTRACT

Dendronised poly(2-oxazoline) hybrid membranes were prepared by solution impregnation and phase inversion precipitation. Dielectric Thermal Analysis (DETA) was used to investigate the effect of the annealing temperature on the dielectric properties of these Side-Chain Liquid-Crystalline Polymers (SCLCPs). Independent of the different thermal treatments, the poly(2-oxazoline) hybrid membranes show similar dielectric spectra containing the same four relaxation mechanisms (γ-, α_{Tg}-, α_{Clear}-, and ρ-relaxation). The thermal orientation reduces the activation energy of the γ-relaxation, by modifying the steric hindrance of the associated aliphatic side chains. Aligning the polymer chains to each other, due to thermal annealing, leads to a less fragile structure. This reduced cooperativity decreases the temperature of the α_{Tg}-relaxation, related to the glass transition. The highly ordered structure of the oriented membranes increases the activation energy and temperature of the α_{Clear}-relaxation, associated with the freeing movement of the mesogenic side groups, especially in the homeotropically aligned membrane. The random orientation decreases the electron conductivity and its thermal activation, while the homeotropic alignment results in an increase, due to the orientation of the columns. The thermal orientation of SCLCPs leads to differences in the temperature dependence and cooperativity of the molecular relaxations and the conductive properties, providing valuable insights into their molecular structure and arrangement.

1. Introduction

For many years, the majority of Proton Exchange Membrane Fuel Cells (PEMFCs) are utilising perfluorosulfonic acid polymers, such as Nafion®, due to their excellent conductive properties and high stability [1]. However, their high production costs, alcohol crossover problem, limited operating temperature (0–100 °C), and water management issues [2,3] are driving researchers to seek alternative solutions.

Side-Chain Liquid-Crystalline Polymers (SCLCPs) have attracted a great deal of interest in recent years due to their unique properties associated with their combined state between an isotropic liquid and an ordered crystal [4]. Typically, the structure of SCLCPs consists of a polymer chain and comb-like mesogenic groups that are attached through flexible spacers [5]. The spacer decouples the motions of the mesogenic group from those of the polymer backbone, enabling the formation of the mesophase [6]. Due to the aromatic moieties in the dendron groups, they can self-assemble into columnar structures with internal channels that are capable of selectively transporting ions [7–9].

In SCLCPs, the main chain containing heteroatoms such as oxygen or nitrogen can provide a permeation pathway for proton hopping without the need for water [10]. This could lead to high anhydrous proton conductivity, simplify the water management, and increase the temperature of operation of PEMFCs. The homeotropic alignment of the columns perpendicular to the substrate surface can further enhance the proton transport in SCLCPs, due to the optimised arrangement of the ionic channels [11].

A detailed study of the dielectric properties of liquid crystal polymers is important to understand their unique behaviour and to expand their range of applications. Dielectric Thermal Analysis (DETA) is a suitable technique to study the thermal activation and cooperativity of molecular dynamics and provide valuable information about the molecular structure and arrangement of SCLCPs [12].

During the last decade the authors have investigated the influence of dendron amount, spacer flexibility, and thermal orientation on the

* Corresponding author.
E-mail address: aribes@ter.upv.es (A. Ribes-Greus).

https://doi.org/10.1016/j.reactfunctpolym.2025.106268
Received 14 October 2024; Received in revised form 24 February 2025; Accepted 14 March 2025
Available online 16 March 2025

dielectric properties of SCLCPs based on poly[2-(aziridin-1-yl)ethanol] (PAZE) [13,14] and poly(epichlorohydrin) (PECH) [15–17]. In each study, modification of the polymer chain with the tapered unit 3,4,5-tris [4-(n-dodecan-1-yloxy)bezyloxy] leads to liquid crystal behaviour, resulting in columnar structures. The heteroatoms situated in the polymer backbone have been shown to successfully form a permeation path along the columns, facilitating cation transport. In particular, the nitrogen-containing SCLCPs based on polyamines show high proton conductivities, although they exhibit poor mechanical properties. The studies highlighted the importance of the order and regularity of the tapered dendron, the effect of the spacer, and the proper thermal annealing to achieve a homeotropic alignment of the columns. Thermal orientation is fundamental for optimizing the anisotropic charge transport properties of SCLCPs, yet its precise influence at the molecular level requires further investigation.

In this study, a different Side-Chain Liquid-Crystalline Polymer is synthesised from the monomer 2-(3,4,5-tris(4-dodecyloxybenzyloxy) phenyl)-4,5-dihydro-1,3-oxazole (TAPOx), which is expected to offer several advantages:

i) The oxazoline unit allows performing a living ring-opening polymerisation in which a narrow molar mass distribution can be achieved by precise control of the reaction's advance [18].
ii) It has a tapered group on each repeating unit and allows for the formation of a polymer with a highly regular structure [19].
iii) It has nitrogen in the polymer backbone which should allow for good proton transport due to its proton donor capabilities [20].

Poly(2-(3,4,5-tris(4-dodecyloxybenzyloxy)phenyl)-2-oxazoline) has been synthesised with a degree of polymerisation of 40. Due to the dendronised poly(2-oxazoline)'s poor mechanical properties, it was incorporated into a polyester support by solution impregnation. Three dendronised poly(2-oxazoline) hybrid membranes were prepared from the same polymer batch, each subjected to different thermal orientation treatments: One membrane remained unoriented, while the other two were oriented at distinct annealing temperatures. Compared to other dielectric studies on SCLCPs, the chemical composition of these samples is identical, with structural differences arising only from their orientation treatment. This allows for an isolated investigation of how polymer column alignment influences dielectric properties. Thermal annealing may modify the orientation of the polymer chain and the mesogenic side groups, potentially altering the dielectric behaviour and molecular relaxation mechanisms. Comprehensive dielectric characterisation of the liquid-crystalline poly(2-oxazoline) membranes was performed to study their self-assembly and thermal orientation at the molecular level, in order to understand their ion-transport properties.

2. Experimental

2.1. Materials

The monomer 2-(3,4,5-tris(4-dodecyloxybenzyloxy)phenyl)-4,5-dihydro-1,3-oxazole (TAPOx) was synthesised by the authors of this work [21]. Methyl trifluoromethanesulfonate (MeOTf, ≥98 %), chlorobenzene (≥99 %), and tetrahydrofuran (THF, ≥99 %, 250 ppm BHT inhibitor) were supplied by Sigma Aldrich (St. Louis, USA). Morpholine (99 %) was purchased from Alfa Aesar (Haverhill, USA). Potassium hydroxide (KOH, 90 %) was acquired from Scharlab (Barcelona, Spain). The polyester fabric used as a support is Hollytex® (22 g/cm^2).

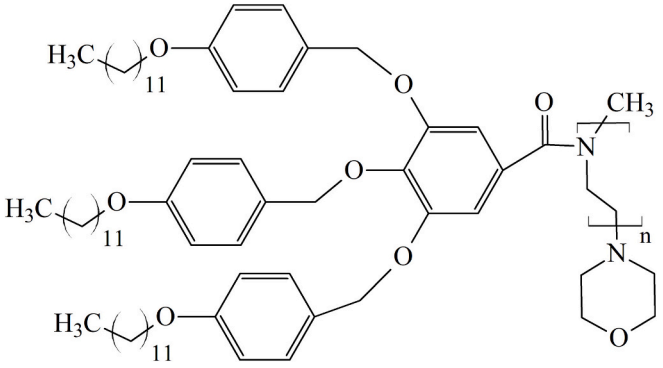

Fig. 1. Chemical structure of dendronised poly(2-oxazoline).

Table 1
Annealing temperature used during thermal treatment and orientation of the dendronised poly(2-oxazoline) hybrid membranes.

Membranes	Annealing temperature (°C)	Orientation
PTOx	–	–
PTOx RO	73	Random
PTOx HO	69	Homeotropic

2.2. Preparation of hybrid poly(2-oxazoline) membranes

The preparation of the Side-Chain Liquid-Crystalline Polymer (SCLCP) poly(2-(3,4,5-tris(4-dodecyloxybenzyloxy)phenyl)2-oxazoline) is described in detail elsewhere [22]. In summary, the monomer TAPOx was melted at 105 °C and then dry chlorobenzene was added to reach a concentration of 1.0 M. Next, a specific amount (0.135 M) of the initiator (MeOTf) was added to achieve a degree of polymerisation (DP) of 40. When the ^{1}H NMR spectrum indicated that the reaction was almost finished (conversion ≥93 %), an excess of the terminating agent morpholine was added. Finally, the mixture was precipitated twice in a cold KOH solution (0.1 M) and dried under vacuum at 50 °C. Fig. 1 shows the chemical structure of dendronised poly(2-oxazoline).

The hybrid poly(2-oxazoline) membranes were prepared by solution impregnation and phase inversion precipitation. First, 50.0 mg of dendronised poly(2-oxazoline) was dissolved in THF to reach a concentration of 30 wt%. The solution was then poured over the polyester support (Ø = 20 mm), that was placed on top of glass substrates. The impregnated fabrics were immersed in a Milli-Q water bath for 15 min and then dried at air overnight. The prepared poly(2-oxazoline) hybrid membranes had a thickness of 220 ± 10 μm and a density of approximately 1.18 g/cm^3.

2.3. Thermal orientation of the membranes

The liquid-crystalline poly(2-oxazoline) hybrid membranes, prepared from the same polymer batch, were subjected to different thermal treatments to achieve homeotropic alignment of the columns. The hybrid membranes were placed on a Linkam Scientific (Redhill, UK) TP92 temperature measurement stage and heated to 150 °C, well above the clearing temperature of dendronised poly(2-oxazoline) (T_{Clear} = 74 °C) [22]. They were kept at this temperature for 30 min before cooling down (0.5 K/min) to the annealing point. Different annealing temperatures were chosen for the membranes to study the influence on the columnar orientation. Table 1 lists the three poly(2-oxazoline)

hybrid membranes of this study, the annealing temperature used during thermal treatment, and the orientation achieved. After 24 h the hybrid membranes were slowly cooled (0.1 K/min) to room temperature.

Guardià et al. investigated the orientation of the dendronised poly(2-oxazoline) membranes of this study using X-ray Diffraction (XRD) [20]. They observed homeotropic alignment of mesogenic poly(2-oxazoline) when annealed at 69 °C (PTOx HO). In contrast, the membrane PTOx RO annealed at 73 °C, did not achieve homeotropic alignment and instead showed a broad peak in the azimuthal XRD scan, possibly due to random orientation of the columns. The annealing temperature of 73 °C was too close to the clearing transition of dendronised poly(2-oxazoline) (T_{Clear} = 74 °C), providing an excess of energy [22]. This may have exceeded the level required for homeotropic alignment, preventing the columns from reaching equilibrium and leading to a random orientation.

2.4. Physico-chemical characterisation

2.4.1. Dielectric Thermal Analysis (DETA)

Dielectric measurements of the dendronised poly(2-oxazoline) hybrid membranes were conducted in a Broadband Dielectric Impedance Spectrometer from Novocontrol Technologies GmbH & Co. KG (Montabaur, Germany). The sample membranes were placed between two stainless-steel electrodes (10 mm diameter) and mounted in the BDS 1200 dielectric test cell. A frequency range from 10^{-2} Hz to 10^{7} Hz with up to 10 points per decade was screened with the Alpha A analyser. Measurements were performed under isothermal conditions in increasing 10 °C steps ranging from −130 °C to 150 °C using the QUATRO Cryosystem. An inert nitrogen atmosphere was used to avoid sample oxidation. The software WinFIT (3.4) from Novocontrol was used for the acquisition and processing of the dielectric data.

2.5. Theory section

The dielectric properties of the liquid-crystalline poly(2-oxazoline) hybrid membranes in this work were analysed in terms of the real and imaginary part of the permittivity (ε', ε''), the loss factor ($\tan(\delta)$), and the imaginary part of the electric modulus (M''). The dielectric relaxations were obtained by deconvoluting the ε''-spectra using Havriliak-Negami functions, employing the Charlesworth method [23,24]. The mode relaxation times (τ_{max}) were obtained from the peak of each relaxation process at each temperature following the deconvolution.

These relaxation times, represented as maximum frequency ($f_{max} = 1/(2{\cdot}\pi{\cdot}\tau_{max})$, are plotted against the reciprocal temperature in an Arrhenius map. Linear processes are fitted to the Arrhenius function, and processes with a non-linear temperature dependence are fitted to the Vogel–Fulcher–Tammann–Hesse (VFTH) function, according to Eqs. (1) and (2), respectively [25].

$$f_{max} = f_0 \cdot exp\left(\frac{-E_a}{R \cdot T}\right) \tag{1}$$

where f_0 is a pre-exponential factor, E_a is the apparent activation energy, and R is the universal gas constant (R = 8.314 J·K^{-1}·mol^{-1}).

$$f_{max} = f_0 \cdot exp\left(\frac{-D \cdot T_V}{T - T_V}\right) \tag{2}$$

where T_V is the Vogel temperature, and D is the fragility parameter, describing the deviation from a linear temperature dependency.

In addition, the VFTH fit permits the determination of the thermal expansion coefficient (α), according to Eq. (3) [26,27].

$$\alpha = \frac{1}{D \cdot T_V} \tag{3}$$

To study the macromolecular nature of the dielectric relaxations, the Eyring model at 1 Hz was applied (Eq. 4) [28].

$$E_a = R \cdot T \cdot [22.92 + ln(T)] \tag{4}$$

In this model, intramolecular relaxations that exhibit no interactions with neighbouring entities fall close to the zero-entropy line. In contrast, relaxations of intermolecular origin involve interactions with neighbours, resulting in cooperative effects and an increase in activation energy.

The electron conductivity of the dendronised poly(2-oxazoline) membranes can be studied by applying Jonscher's power law (Eq. 5) to the modulus of the conductivity ($|\sigma|$) [29]:

$$\sigma(\omega) = \sigma_{dc} + A\omega^n \tag{5}$$

where σ_{DC} is the direct current (DC) conductivity and $A\omega^n$ is the alternating current (AC) conductivity component, where A is a pre-exponential constant and n is the fractional exponent in the range $0 < n \leq 1$. At low frequencies the AC component is absent and the frequency-independent electron conductivity (σ_{elec}) can be determined from the DC plateau [30].

3. Results and discussion

3.1. Dielectric analysis of dendronised poly(2-oxazoline) hybrid membranes

3.1.1. Phenomenological analysis of the dielectric spectra

The dielectric spectra of the liquid crystal poly(2-oxazoline) hybrid membranes are represented in three-dimensional plots of the imaginary part of the permittivity (ε'') and isochronal plots of the imaginary part of the electric modulus (M'') in Fig. 2.

The poly(2-oxazoline) hybrid membranes show a similar three-dimensional imaginary permittivity (ε'') spectrum with the same characteristics, regardless of their different thermal treatment. The imaginary part of the electric modulus (M'') masks the conductivity contribution at high temperatures and provides improved isolation of the relaxation processes [31].

The three dendronised poly(2-oxazoline) materials show the same four relaxation mechanisms in the dielectric spectra between −130 °C and 150 °C. The detected processes were assigned the names γ-relaxation, α_{Tg}-relaxation, α_{Clear}-relaxation, and ρ-relaxation, in order of increasing temperature. These molecular relaxations were also found by our research group for similar LCSCPs, containing the same mesogenic side group [13,15–17].

The γ-relaxation is attributed to local motions of the aliphatic terminal chain connected to the benzyloxy group of the dendrimer side group. The α_{Tg}-relaxation represents the glass-rubber transition of the poly(2-oxazoline) membranes, through which the polymer segments can begin to rearrange. Subsequently, the α_{Clear}-relaxation is related to the freeing motions of the entire mesogenic side group around its short axis [12]. This relaxation is closely related to the clearing transition of the mesophase, where the columnar structure of the polymer gets disassembled, due to the thermally induced motions of the mesogenic group. As a result, the polymers lose their liquid crystalline (smectic)

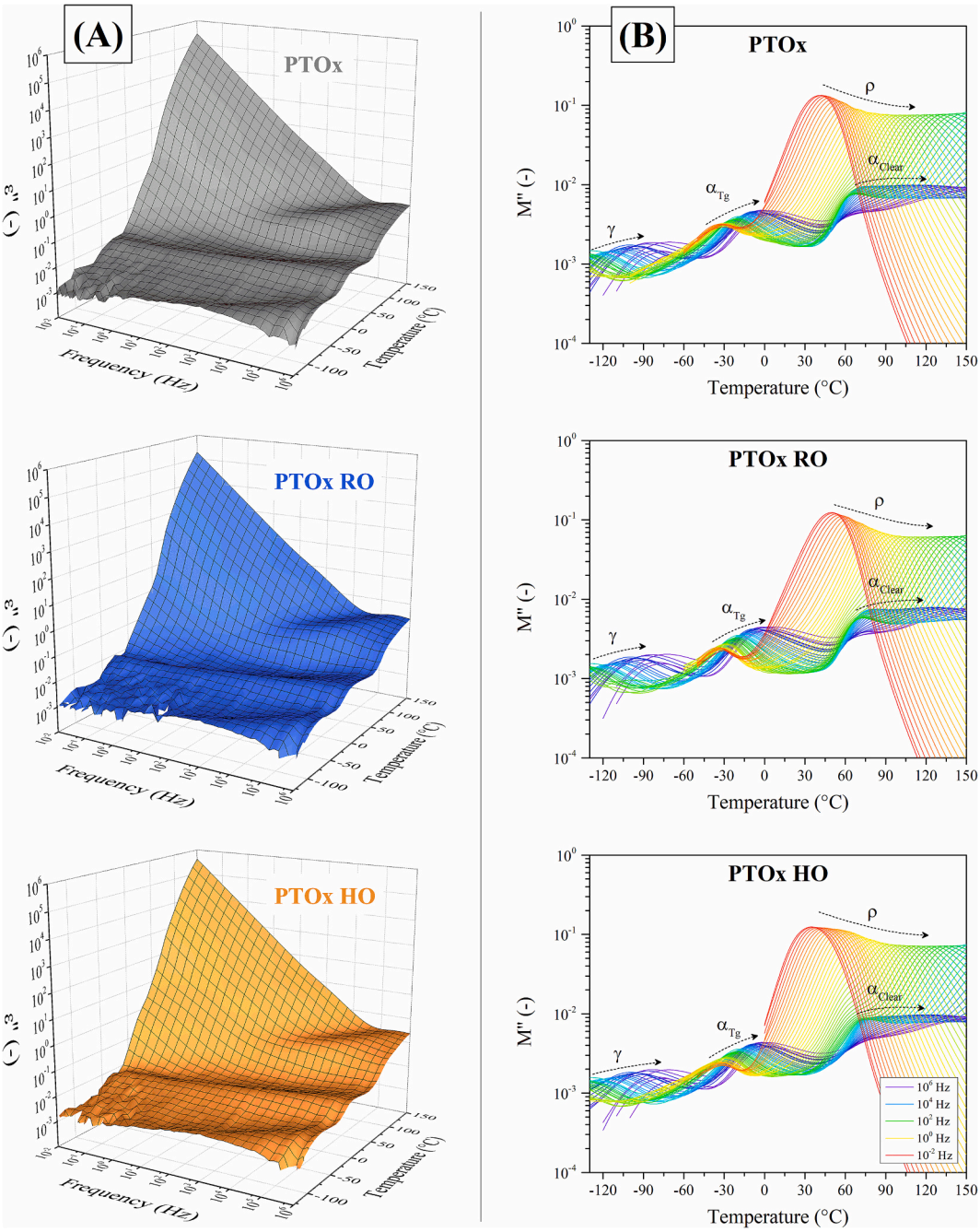

Fig. 2. (A) 3D plots of the imaginary part of the permittivity (ε'') and (B) isochronal plots of the imaginary electric modulus (M'') of the dendronised poly(2-oxazoline) membranes.

order and become isotropic.

At high temperatures, another ρ-relaxation can be found in the low-frequency region, which is attributed to a Maxwell-Wagner-Sillars (MWS) polarisation. This interfacial polarisation is typically found in heterogeneous materials where charges can accumulate at boundaries between two regions with different permittivity [12].

Fig. 3 represents the structure of dendronised poly(2-oxazoline) and the main dielectric relaxation mechanisms, as well as the proposed structural parts to which they belong. In addition, the figure includes a schematic representation of the self-assembly of liquid-crystalline poly (2-oxazoline) into a columnar structure and the homeotropic alignment due to thermal orientation.

3.1.2. *Cooperativity of the dielectric relaxations*

In order to understand the structural conformation of the different poly(2-oxazoline) membranes, the spectra of the imaginary permittivity (ε'') were deconvoluted with Havriliak–Negami (HN) functions to obtain the relaxation times of each process [23]. Furthermore, the cooperativity of the dielectric relaxations is investigated according to the Eyring model (Eq. 4) [28]. Assuming a linear relation between the relaxation time and inverse temperature, the activation energy (E_a) was calculated for each of the previously mentioned processes and is represented in Fig. 4.

As can be appreciated in the Eyring plot, the α_{Clear}-relaxation exhibits two linear regions, one below the clearing transition ($\alpha_{Clear,I}$) and another one above ($\alpha_{Clear,II}$). The side-chain liquid-crystalline poly(2-oxazoline) membranes show three processes (γ-, $\alpha_{Clear,II}$, and

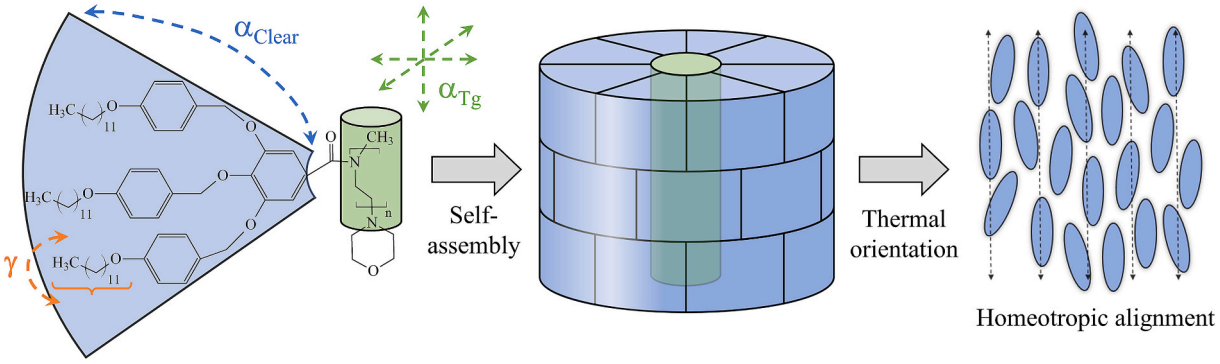

Fig. 3. Main dielectric relaxation processes as well as schematic representation of the self-assembly and homeotropic alignment of dendronised poly(2-oxazoline).

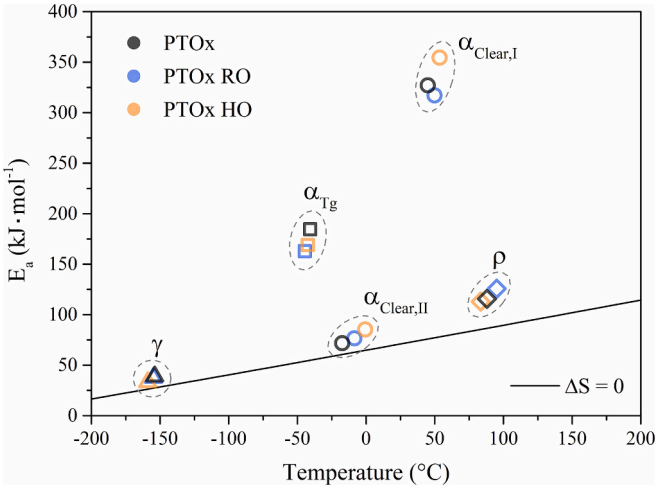

Fig. 4. Eyring plot of the relaxation mechanisms of the dendronised poly(2-oxazoline) hybrid membranes at 1 Hz.

ρ-relaxation) close to the zero-entropy line and two processes (α_{Tg}- and $\alpha_{Clear,I}$-relaxation) with a significant deviation.

Local motions, such as the γ-relaxation, are usually not sterically hindered by neighbouring entities and do not have a cooperative effect. However, relaxations representing phase transitions such as the glass transition (α_{Tg}) typically show a cooperative contribution. The motion of a segment is constrained by both intramolecular and intermolecular interactions, due to the connectivity of the polymer chain and the steric hindrance from neighbouring segments [32]. Likewise, the α_{Clear}-relaxation below the clearing transition temperature ($\alpha_{Clear,I}$, $T < 74$ °C) displays a cooperative contribution because the liquid-crystalline poly(2-oxazoline) membranes are in the smectic phase where the molecules are strongly ordered. This highly crystalline state restricts the rotational and translational mobility leading to an increased activation energy of the α_{Clear}-motion [12]. After undergoing the clearing transition ($\alpha_{Clear,II}$, $T > 74$ °C), the polymer becomes isotropic, and the relaxation significantly loses its cooperativity.

3.1.3. *Analysis of the γ-relaxation*

For all the poly(2-oxazoline) hybrid membranes, the γ-relaxation was found at in the scanned frequency range between −130 °C and −70 °C. Fig. 5-(A) shows the isochronal plot of the imaginary permittivity (ε'') at 10^5 Hz of the membranes.

The peak of the three poly(2-oxazoline) membranes occurs at the same temperature in the isochronal plot and shows a comparable relaxation time distribution. However, the thermal orientation increases the height of the peak, which is more prominent in the homeotropic

Table 2
Arrhenius fit values of the γ-relaxation of the dendronised poly(2-oxazoline) membranes.

	γ-relaxation		
	T_{1Hz} (°C)	E_a (kJ/mol)	R^2
PTOx	−153.9	39.0	0.998
PTOx RO	−154.7	37.6	0.997
PTOx HO	−158.9	33.3	0.994

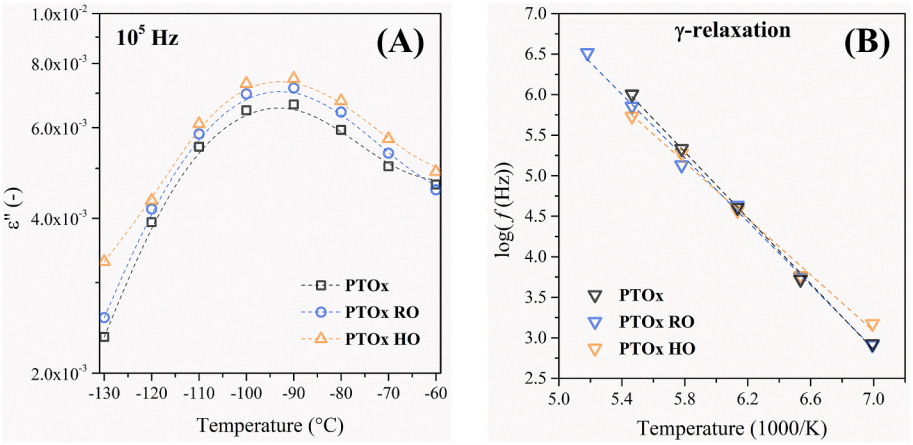

Fig. 5. (A) Isochronal plot of the imaginary part of the permittivity (ε'') at 10^5 Hz and (B) Arrhenius map of the γ-relaxation of the dendronised poly(2-oxazoline) hybrid membranes.

aligned membrane (PTOx HO) than in the random oriented membrane (PTOx RO).

Fig. 5-(B) represents the relaxation time of the γ-relaxation as a function of inverse temperature. A linear temperature dependence of the γ-relaxation was found and was therefore adjusted to the Arrhenius model (Eq. 1), with the results of the fit being summarised in Table 2.

The three dendronised poly(2-oxazoline) membranes show activation energies between 33.3 and 39.0 kJ/mol, typical of local molecular arrangements of intramolecular nature. These E_a-values are comparable with the results obtained for liquid crystal poly(epichlorohydrin) (PECH) [17] and poly[2-(aziridin-1-yl)ethanol] (PAZE) membranes [13], containing the same dendrimer unit. According to these findings, the γ-relaxation is associated to motions of the terminal aliphatic chain of the mesogenic side unit. However, in contrast to the PECH and PAZE materials, the activation energy of dendronised poly(2-oxazoline) membranes decreases with thermal orientation.

The dendronised poly(2-oxazoline) membranes of this study have a shorter spacer length in comparison to the PECH and PAZE materials. The spacer connects the mesogenic unit with the polymer backbone and its length has an important influence on the mobility of the SCLCPs components [6]. The shorter spacer length of the poly(2-oxazoline) membranes in this study leads to a slightly increased activation energy of the γ-relaxation, due to the steric hindrance and less flexible side group.

The homeotropic and random orientation of the liquid-crystalline poly(2-oxazoline) membranes reduces the steric hindrance of the mesogenic side groups as they seek maximum distance between each other. Therefore, the aliphatic terminal chains are less constrained and more mobile, requiring less energy to induce the related γ-relaxation. This effect is stronger for the homeotropic oriented membrane (PTOx HO) annealed at 69 °C in comparison to the random oriented membrane (PTOx RO), because its annealing temperature of 73 °C is closer to the clearing transition (T_{Clear} = 74 °C) [20].

3.1.4. Analysis of the α_{Tg}-relaxation

The α_{Tg}-relaxation, commonly attributed to the glass transition of the polymer, is found between −50 °C and 40 °C for the three poly(2-oxazoline) membranes. Fig. 6-(A) shows the isochronal plot of the imaginary part of the permittivity (ε'') plot at 10^4 Hz. In addition, the plot include the calorimetric glass transition of dendronised poly(2-oxazoline) (T_g = −12 °C) [22].

The α_{Tg}-relaxation peak of the dendronised poly(2-oxazoline) membranes at a frequency of 10^4 Hz falls within a similar temperature range as the calorimetric glass transition. The thermal treatment orients the polymer chains, which slightly shifts the α_{Tg}-relaxation to lower temperatures and reduces the peak height. Zhong et al. likewise found a reduction of dielectric strength of the glass transition of SCLCPS by homeotropic alignment [5,6].

Table 3
VFTH fit values of the α_{Tg}-relaxation of the dendronised poly(2-oxazoline) membranes.

	α_{Tg}-relaxation				
	T_V (K)	$log(f_0)$	D	$\alpha \cdot 10^4$	R^2
PTOx	251.4 ± 0.7	6.89 ± 0.06	0.36 ± 0.03	109.6	0.998
PTOx RO	236.9 ± 0.5	7.49 ± 0.04	0.62 ± 0.03	68.4	0.999
PTOx HO	237.5 ± 1.3	7.68 ± 0.12	0.66 ± 0.08	64.2	0.997

Fig. 6-(B) plots the relaxation time of the α_{Tg}-relaxation of the dendronised poly(2-oxazoline) membranes in an Arrhenius map. A non-linear temperature dependency was found for the α_{Tg}-relaxation, confirming the assignment to the glass-rubber transition. Accordingly, the dendronised poly(2-oxazoline) hybrid membranes are adjusted to the VFTH function (Eq. 2). Table 3 contains the Vogel temperature (T_V), relaxation frequency ($log(f_0)$), the dynamic fragility parameter (D), and the thermal expansion coefficient (α) from the VFTH fit.

The dendronised poly(2-oxazoline) membranes exhibit Vogel temperatures (T_V) between 236.9 and 251.4 K. The Vogel temperature describes the behaviour of polymers near the glass transition and is typically 40 K lower than the calorimetric T_g [12]. Accordingly, the dielectric glass transition ($T_{g,dielectric}$) of the poly(2-oxazoline) membranes occurs between 3.8 and 18.3 °C, which is slightly higher than the calorimetric value ($T_{g,calorimetric}$) of −12 °C [22].

The dynamic fragility parameter (D) measures the fragility of materials. According to the classification by Angell, all three poly(2-oxazoline) membranes of this study can be considered fragile materials ($D < 6$) [33]. Fragile materials exhibit abrupt changes in their physical properties as they approach the glass transition. However, the homeotropic and random orientation of the hybrid membranes makes the mesogenic poly(2-oxazoline) slightly less fragile, as can be seen in the increase of the D-values. In addition, the α_{Tg}-relaxation of the homeotropically and randomly oriented poly(2-oxazoline) membrane shows a higher relaxation frequency ($log(f_0)$) and a lower Vogel temperature (T_V) compared to the unoriented membranes. The same results were found for homeotropically oriented polyvinyl-ether-based cyanobiphenyl SCLCPs [5].

The thermal treatment applied to the liquid-crystalline poly(2-oxazoline) aligns the polymer segments towards each other and therefore reduces the cooperativity between the chains. This justifies the displacement of the α_{Tg}-relaxation towards lower temperatures, the lower thermal expansion coefficient (α), and the slight reduction of cooperativity found in the Eyring plot (see Fig. 4).

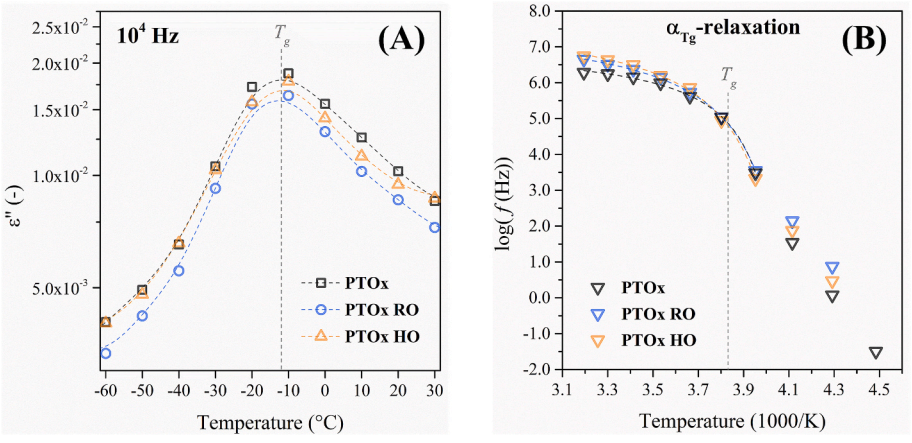

Fig. 6. (A) Isochronal plot of the imaginary part of the permittivity (ε'') at 10^4 Hz and (B) Arrhenius map of the α_{Tg}-relaxation.

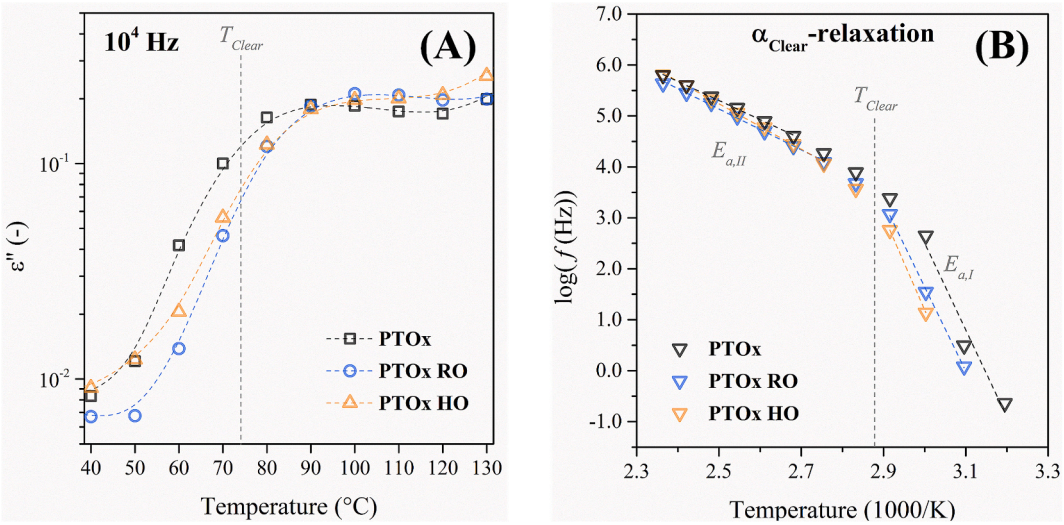

Fig. 7. (A) Isochronal plot of the imaginary part of the permittivity (ε'') at 10^4 Hz and (B) Arrhenius map of the α_{Clear}-relaxation.

Table 4
Arrhenius fit values of the low-temperature and high-temperature zone of the α_{Clear}-relaxation of the dendronised poly(2-oxazoline) membranes.

	$\alpha_{Clear,1}$-relaxation ($T < T_{Clear}$)		
	T_{1Hz} (°C)	E_a (kJ/mol)	R^2
PTOx	44.9	327.1	0.962
PTOx RO	49.8	317.1	0.999
PTOx HO	53.5	354.5	1.0[a]

	$\alpha_{Clear,2}$-relaxation ($T > T_{Clear}$)		
	T_{1Hz} (°C)	E_a (kJ/mol)	R^2
PTOx	−17.4	71.9	0.999
PTOx RO	−8.5	76.7	0.997
PTOx HO	−0.7	85.5	0.998

[a] Only 2 points taken for fit.

3.1.5. *Analysis of the α_{Clear}-relaxation*

The α_{Clear}-relaxation of the dendronised poly(2-oxazoline) hybrid membranes was found in the analysed frequency range between 40 °C and 150 °C. Fig. 7-(A) shows the isochronal plot of the imaginary permittivity (ε'') at 10^4 Hz of these membranes including the calorimetric clearing transition of dendronised poly(2-oxazoline) (T_{Clear} = 74 °C) [22].

The peak of the α_{Clear}-relaxation at a frequency of 10^4 Hz is in close proximity to the calorimetric clearing transition of dendronised poly(2-oxazoline) and is therefore assigned to the freeing movements of the entire mesogenic side group around its short axis. These motions are responsible for the clearing transition of the liquid-crystalline polymers, as they disassemble the columnar structure and turn isotropic. The homeotropic and random orientation shifts the relaxation peak towards high temperatures and slightly increases the peak height.

The relaxation time of the α_{Clear}-relaxation as a function of inverse temperature is represented in an Arrhenius map in Fig. 7-(B). Linear temperature dependence was found for the α_{Clear}-relaxation with a significant change in slope around the calorimetric clearing transition, likewise found for other Side-Chain Liquid-Crystalline Polymers [34–39]. Accordingly, the linear dependency of both zones was adjusted to the Arrhenius model (Eq. 1), with the results of the fit being summarised in Table 4. The activation energy of the α_{Clear}-relaxation before the clearing transition shows an activation energy of around 330 kJ/mol. It has to be noted, that only a few data points in this zone could be taken for the fit, due to the high thermal activation of the relaxation process and due to overlapping with the ρ-relaxation at low frequencies.

The α_{Clear}-relaxation of the dendronised poly(2-oxazoline) membranes above the clearing transition shows activation energies between 71.9 and 85.5 kJ/mol. The thermal activation and the temperature of this relaxation process increase as a function of the orientation degree.

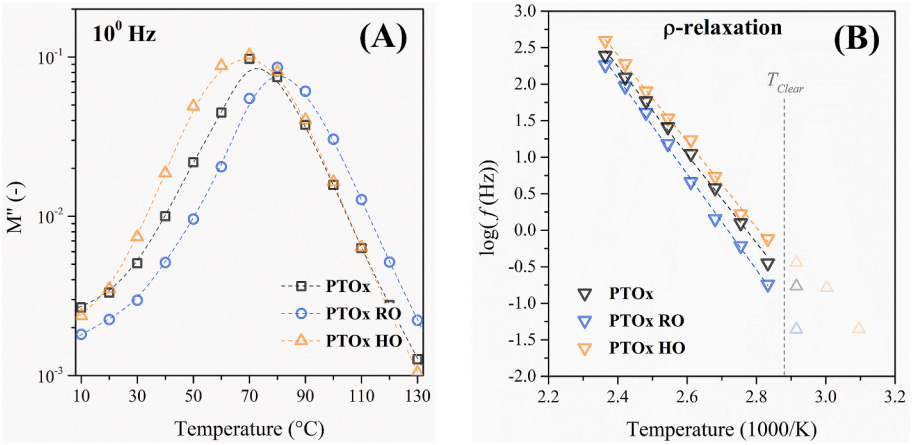

Fig. 8. (A) Isochronal plot of the imaginary part of the electric modulus (M'') at 10^0 Hz and (B) Arrhenius map of the ρ-relaxation.

Table 5
Arrhenius fit values of the ρ-relaxation of the dendronised poly(2-oxazoline) membranes.

	ρ-relaxation		
	T_{1Hz} (°C)	E_a (kJ/mol)	R^2
PTOx	88.0	115.7	0.997
PTOx RO	95.1	125.7	0.998
PTOx HO	83.5	113.0	0.998

Accordingly, the homeotropically orientated membrane (PTOx HO) results in the highest order structure. Therefore, higher thermal energies need to be overcome to induce the freeing motion of the dendrimer unit [12].

3.1.6. Analysis of the ρ-relaxation

At low frequencies, the three poly(2-oxazoline) membranes show a ρ-relaxation between 50 °C and 150 °C. Fig. 8-(A) shows the isochronal plot of the imaginary part of the electric modulus (M'') at 10^0 Hz. In contrast to the other molecular relaxations, the imaginary modulus (M'') was chosen to see the ρ-relaxation, as the imaginary permittivity (ε'') at these frequencies is overlapped by the conductivity contribution.

The ρ-relaxation of a similar SCLCPs based on poly[2-(aziridin-1-yl) ethanol] (PAZE) was also observed in the same temperature and frequency range [13] and was assigned to a Maxwell-Wagner-Sillars (MWS) polarisation, resulting from the accumulation of charges at interfaces with different conductivity. The peaks of the ρ-relaxation of the three dendronised poly(2-oxazoline) hybrid membranes occur at different temperatures in the order PTOx RO > PTOx > PTOx HO.

Fig. 8-(B) represents the relaxation time of the ρ-relaxation as a function of inverse temperature and the calorimetric clearing transition (T_{Clear} = 74 °C) [22]. The linear temperature dependence was adjusted to the Arrhenius model (Eq. 1), with the results of the fit being summarised in Table 5. The points after the calorimetric clearing transition were taken for the fit because the data at lower temperatures converge with the α_{Clear}-relaxation.

The dendronised poly(2-oxazoline) membranes show activation energies ranging from 113 to 126 kJ/mol, typical values for interfacial MWS polarisations [40]. The values for the activation energy of the ρ-relaxation follow the same order as the temperature: PTOx RO > PTOx > PTOx HO.

3.1.7. Electron conductivity

Furthermore, the electron conductivity of the dendronised poly(2-oxazoline) hybrid membranes is investigated. Fig. 9 represents the modulus of the electric conductivity ($|\sigma|$) between 0 °C and 150 °C.

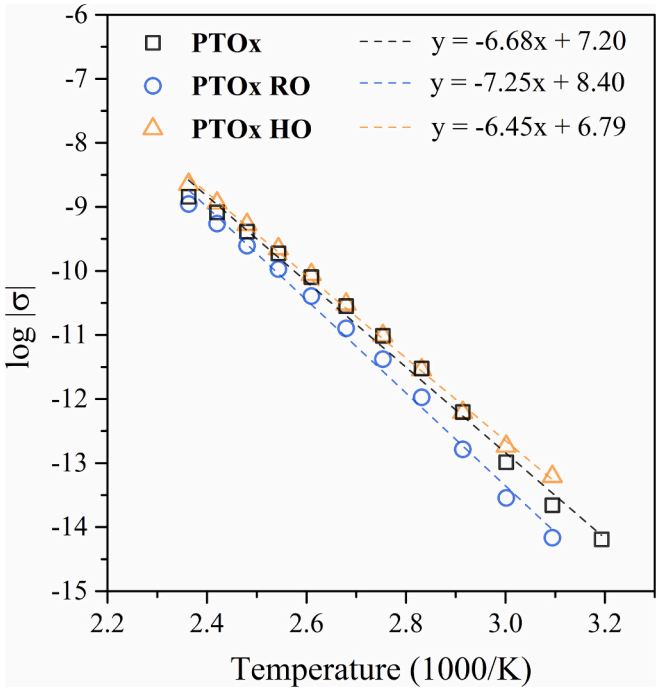

Fig. 10. Arrhenius map of the electron conductivity ($|\sigma|$) of the dendronised poly(2-oxazoline) hybrid membranes.

Table 6
Activation energy from the Arrhenius fit of the electric bulk conductivity of the dendronised poly(2-oxazoline) membranes.

	Intercept	Slope	E_a (kJ/mol)	R^2
PTOx	7.20	−6.68	127.9	0.993
PTOx RO	8.40	−7.25	138.8	0.998
PTOx HO	6.79	−6.45	123.5	0.993

The three mesogenic poly(2-oxazoline) membranes show a comparable curve progression, with a plateau at low frequencies and a steep linear increase towards higher frequencies. The curves were adjusted to Jonscher's power law in order to obtain the frequency-independent DC plateau, representing the bulk conductivity (σ_0) of the materials.

The obtained bulk conductivity of the dendronised poly(2-oxazoline) membranes is represented as a function of inverse temperature in Fig. 10.

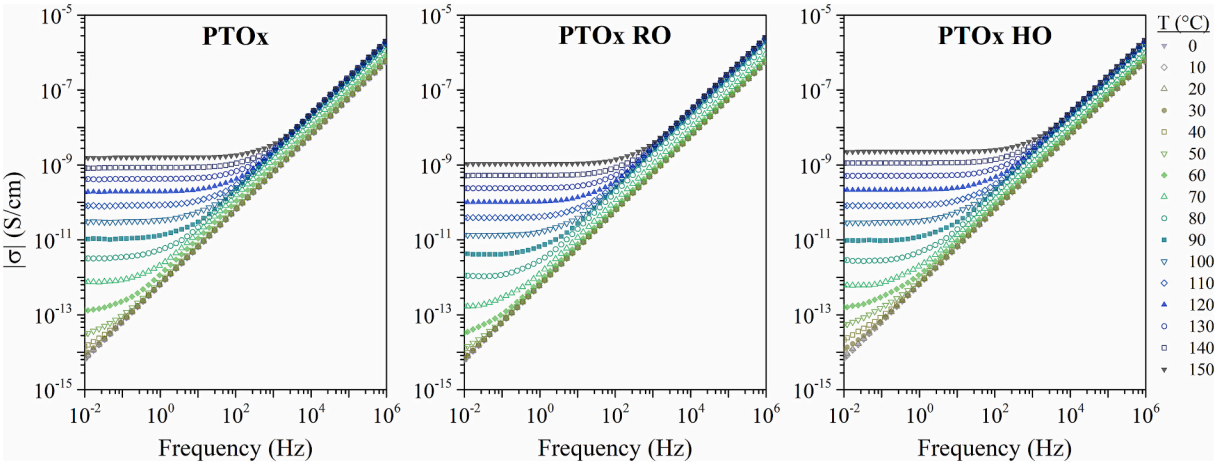

Fig. 9. Modulus of the conductivity ($|\sigma|$) of the dendronised poly(2-oxazoline) hybrid membranes.

The poly(2-oxazoline) hybrid membranes show low electric conductivities between 10^{-15} S/cm to 10^{-8} S/cm between 40 °C and 150 °C. The values show the ability of the liquid-crystalline poly(2-oxazoline) hybrid membranes to act as electrical insulators, for example in fuel cells. The linear temperature dependence found for the electron conductivity was adjusted to the Arrhenius model, with the results summarised in Table 6.

The thermal activation of the electron conductivity of the dendronised poly(2-oxazoline) hybrid membranes is between 123.5 and 138.8 kJ/mol. These E_a-values are very similar to the activation energies obtained from the ρ-relaxation and show the same differences between the membranes, in increasing order: PTOx RO > PTOx > PTOx HO. Khan et al. also found in poly(amidoamine) dendrimers a close relationship between the electron conductivity and MWS polarisation [41]. According to the results, the randomly oriented membrane PTOx RO, annealed at 73 °C, exhibits the lowest electron conductivity and thermal activation. In contrast, the homeotropic aligned membrane PTOx HO, annealed at 69 °C, results in the highest electron conductivity, due to the orientation of the columns.

4. Conclusions

The dielectric spectra of the liquid-crystalline poly(2-oxazoline) hybrid membranes of this study reveal the same four dielectric relaxation mechanisms, despite the different thermal treatments applied: A local γ-relaxation, due to motions of the aliphatic chain of the mesogenic side group, the α_{Tg}-relaxation, representing the segmental glass transition, the α_{Clear}-relaxation related to motions of the entire mesogenic side group, and ultimately a ρ-relaxation, due to an interfacial Maxwell-Wagner-Sillars (MWS) polarisation.

The short spacer length of the dendronised poly(2-oxazoline) membranes leads to a restricted and immobile side group. The thermal orientation reduces this steric hindrance as they seek maximum distance between each other, reducing the activation energy of the γ-relaxation. This effect is stronger in the homeotropic-oriented membrane.

The thermal annealing aligns the polymer main chains to each other, reducing the cooperative contribution of the α_{Tg}-relaxation, related to the segmental motion. The oriented membranes are slightly less fragile and show a reduced dielectric glass transition temperature.

The higher order of the oriented poly(2-oxazoline) membranes increases the activation energy of the α_{Clear}-relaxation, related to the freeing movement of the mesogenic side group, especially in the homeotropic oriented membrane.

The random orientation of the membrane reduces the electron conductivity and its thermal activation. In contrast, the homeotropic alignment leads to an electron conductivity increase, due to the favourable orientation of the columns.

The thermal orientation processes permit to design Side-Chain Liquid-Crystalline Polymers (SCLCPs) with required dielectric and conductive properties.

CRediT authorship contribution statement

Mark Henning Wolf: Writing – original draft, Validation, Methodology, Investigation, Formal analysis. **Jordi Guardià:** Resources, Investigation, Formal analysis. **José Antonio Reina:** Writing – review & editing, Supervision, Conceptualization. **Xavier Montané:** Writing – review & editing, Supervision, Formal analysis, Conceptualization. **Marta Giamberini:** Writing – review & editing, Supervision, Resources, Project administration, Methodology, Funding acquisition, Conceptualization. **Amparo Ribes-Greus:** Writing – review & editing, Supervision, Resources, Project administration, Methodology, Funding acquisition, Conceptualization.

Declaration of competing interest

The authors declare that they have no known competing financial interests or personal relationships that could have appeared to influence the work reported in this paper.

Acknowledgements

This study forms part of the Advanced Materials programme and was supported by the Spanish Ministry of Science and Innovation with funding from European Union NextGenerationEU (PRTR-C17.11) and by Generalitat Valenciana (MFA/2022/041). The authors also thank the Spanish Ministry of Universities for the pre-doctoral FPU grant of M.H. Wolf (FPU21/00853) and the Universitat Rovira i Virgili and Diputació de Tarragona for a pre-doctoral contract (2020PMF-PIPF-21) of J. Guardià within its Martí i Franquès programme.

Data availability

The data supporting the findings of this study cannot be shared at this time as the data also forms part of an ongoing study.

References

[1] T.K. Maiti, J. Singh, P. Dixit, J. Majhi, S. Bhushan, A. Bandyopadhyay, S. Chattopadhyay, Advances in perfluorosulfonic acid-based proton exchange membranes for fuel cell applications: a review, Chem. Eng. J. Adv. 12 (2022) 100372, https://doi.org/10.1016/j.ceja.2022.100372.
[2] M.B. Karimi, F. Mohammadi, K. Hooshyari, Recent approaches to improve Nafion performance for fuel cell applications: a review, Int. J. Hydrog. Energy 44 (2019) 28919–28938, https://doi.org/10.1016/j.ijhydene.2019.09.096.
[3] H. Zhang, P.K. Shen, Recent development of polymer electrolyte membranes for fuel cells, Chem. Rev. 112 (2012) 2780–2832, https://doi.org/10.1021/cr200035s.
[4] J. Guardià, J.A. Reina, M. Giamberini, X. Montané, An up-to-date overview of liquid crystals and liquid crystal polymers for different applications: a review, Polymers (Basel) 16 (2024) 2293, https://doi.org/10.3390/polym16162293.
[5] Z.Z. Zhong, W.L. Gordon, D.E. Schuele, R.B. Akins, V. Percec, Dielectric relaxations of a smectic side-chain liquid-crystalline polymer in different alignment states, Mol. Cryst. Liq. Cryst. Sci. Technol. A Mol. Cryst. Liq. Cryst. 238 (1994) 129–145, https://doi.org/10.1080/10587259408046922.
[6] Z.Z. Zhong, D.E. Schuele, W.L. Gordon, Influence of spacer length on the dielectric relaxation of a side chain liquid crystal polymer, Liq. Cryst. 17 (1994) 199–209, https://doi.org/10.1080/02678299408036560.
[7] X. Montané, S.V. Bhosale, J.A. Reina, M. Giamberini, Columnar liquid crystalline polyglycidol derivatives: a novel alternative for proton-conducting membranes, Polymer (Guildf.) 66 (2015) 100–109, https://doi.org/10.1016/j.polymer.2015.03.071.
[8] H.J. Sun, S. Zhang, V. Percec, From structure to function via complex supramolecular dendrimer systems, Chem. Soc. Rev. 44 (2015) 3900–3923, https://doi.org/10.1039/c4cs00249k.
[9] V. Percec, M. Glodde, T.K. Bera, Y. Miura, I. Shiyanovskaya, K.D. Singer, V.S. K. Balagurusamy, P.A. Heiney, I. Schnell, A. Rapp, H.W. Spiess, S.D. Hudsonk, H. Duan, Self-organization of supramolecular helical dendrimers into complex electronic materials, Nature 417 (2002) 384–387, https://doi.org/10.1038/nature01072.
[10] S. Chai, F. Xu, R. Zhang, X. Wang, L. Zhai, X. Li, H.J. Qian, L. Wu, H. Li, Hybrid liquid-crystalline electrolytes with high-temperature-stable channels for anhydrous proton conduction, J. Am. Chem. Soc. 143 (2021) 21433–21442, https://doi.org/10.1021/jacs.1c11884.
[11] T. Kato, M. Yoshio, T. Ichikawa, B. Soberats, H. Ohno, M. Funahashi, Transport of ions and electrons in nanostructured liquid crystals, Nat. Rev. Mater. 2 (2017) 1–20, https://doi.org/10.1038/natrevmats.2017.1.
[12] F. Kremer, A. Schönhals, Broadband Dielectric Spectroscopy, 2003, https://doi.org/10.1007/978-3-642-56120-7.
[13] R. Teruel-Juanes, K.A. Bogdanowicz, J.D. Badia, V.S. de Juano-Arbona, R. Graf, J. A. Reina, M. Giamberini, A. Ribes-Greus, Molecular mobility in oriented and unoriented membranes based on poly[2-(Aziridin-1-yl)ethanol], Polymers (Basel) 13 (2021) 1–20, https://doi.org/10.3390/polym13071060.
[14] X. Montané, K.A. Bogdanowicz, G. Colace, J.A. Reina, P. Cerruti, A. Lederer, M. Giamberini, Advances in the design of self-supported ion-conducting membranes-new family of columnar liquid crystalline polyamines. Part 1: copolymer synthesis and membrane preparation, Polymer (Guildf.) 105 (2016) 298–309, https://doi.org/10.1016/j.polymer.2016.10.047.
[15] B. Pascual-Jose, A. Zare, S. De la Flor, J.A. Reina, M. Giamberini, A. Ribes-Greus, Dielectric properties in oriented and unoriented membranes based on poly (epichlorohydrin-co-ethylene oxide) copolymers: part III, Polymers (Basel) 14 (2022) 1369, https://doi.org/10.3390/polym14071369.
[16] A. Zare, B. Pascual-Jose, S. De la Flor, A. Ribes-Greus, X. Montané, J.A. Reina, M. Giamberini, Membranes for cation transport based on dendronized poly

(Epichlorohydrin-co-ethylene oxide). Part 1: the effect of dendron amount and column orientation on copolymer mobility, Polymers (Basel) 13 (2021) 3532, https://doi.org/10.3390/polym13203532.
[17] R. Teruel-Juanes, B. Pascual-Jose, R. Graf, J.A. Reina, M. Giamberini, A. Ribes-Greus, Effect of dendritic side groups on the mobility of modified poly (epichlorohydrin) copolymers, Polymers (Basel) (2021) 1–19, https://doi.org/10.3390/polym13121961.
[18] S. Jana, R. Hoogenboom, Poly(2-oxazoline)s: a comprehensive overview of polymer structures and their physical properties—an update, Polym. Int. 71 (2022) 935–949, https://doi.org/10.1002/pi.6426.
[19] M. Glassner, M. Vergaelen, R. Hoogenboom, Poly(2-oxazoline)s: a comprehensive overview of polymer structures and their physical properties, Polym. Int. 67 (2018) 32–45, https://doi.org/10.1002/pi.5457.
[20] J. Guardià Blanch, Columnar Liquid-crystalline Polymers Containing Nitrogen at the Backbone to be Used to Prepare Ion-transport Membranes, Doctoral Thesis for Universitat Rovira i Virgili, 2024.
[21] J. Guardià, A. Zare, J. Eleeza, M. Giamberini, J.A. Reina, X. Montané, Synthesis and characterization of dendritic compounds containing nitrogen: monomer precursors in the construction of biomimetic membranes, Sci. Rep. 12 (2022) 1–17, https://doi.org/10.1038/s41598-022-05747-1.
[22] J. Guardià, M. Giamberini, J.A. Reina, X. Montané, Synthesis and characterization of dendronized side chain liquid crystalline poly(2-oxazoline)s towards biomimetic ion channels, Eur. Polym. J. 196 (2023) 112273, https://doi.org/10.1016/j.eurpolymj.2023.112273.
[23] J.M. Charlesworth, Deconvolution of overlapping relaxations in dynamic mechanical spectra, J. Mater. Sci. 28 (1993) 399–404, https://doi.org/10.1007/BF00357816.
[24] S. Havriliak, S. Negami, A complex plane representation of dielectric and mechanical relaxation processes in some polymers, Polymer (Guildf.) 8 (1967) 161–210, https://doi.org/10.1016/0032-3861(67)90021-3.
[25] G.S. Fulcher, Analysis of recent measurements of the viscosity of glasses, J. Am. Ceram. Soc. 75 (1992) 1043–1055, https://doi.org/10.1111/j.1151-2916.1992.tb05536.x.
[26] Q. Qin, G.B. McKenna, Correlation between dynamic fragility and glass transition temperature for different classes of glass forming liquids, J. Non-Cryst. Solids 352 (2006) 2977–2985, https://doi.org/10.1016/j.jnoncrysol.2006.04.014.
[27] K. Kunal, C.G. Robertson, S. Pawlus, S.F. Hahn, A.P. Sokolov, Role of chemical structure in fragility of polymers: a qualitative picture, Macromolecules 41 (2008) 7232–7238, https://doi.org/10.1021/ma801155c.
[28] H.W. Starkweather, Aspects of simple, non-cooperative relaxations, Polymer (Guildf.) 32 (1991) 2443–2448, https://doi.org/10.1016/0032-3861(91)90087-Y.
[29] A.K. Jonscher, The "universal" dielectric response, Nature 267 (1977) 673–679.
[30] R. Teruel-Juanes, C. del Río, O. Gil-Castell, C. Primaz, A. Ribes-Greus, Triblock SEBS/DVB crosslinked and sulfonated membranes: fuel cell performance and conductivity, J. Appl. Polym. Sci. 138 (2021) 50671, https://doi.org/10.1002/app.50671.
[31] A. Vassilikou-Dova, I.M. Kalogeras, Dielectric Analysis (DEA), 2008, https://doi.org/10.1002/9780470423837.ch6.
[32] K.L. Ngai, C.M. Roland, Chemical structure and intermolecular cooperativity: dielectric relaxation results, Macromolecules 26 (1993) 6824–6830, https://doi.org/10.1021/ma00077a019.
[33] C.A. Angell, Relaxation in liquids, polymers and plastic crystals - strong/fragile patterns and problems, J. Non-Cryst. Solids 131 (1991) 13–31.
[34] W. Haase, H. Pranoto, F.J. Bormuth, Dielectric properties of some side chain liquid crystalline polymers, Ber. Bunsenges./Phys. Chem. Chem. Phys. 89 (1985) 1229–1234, https://doi.org/10.1002/bbpc.19850891122.
[35] H. Kresse, S. Ernst, B. Krücke, F. Kremer, S.U. Vallerien, Comparative dielectric investigations of two liquid-crystalline side chain polymers, Liq. Cryst. 11 (1992) 439–445, https://doi.org/10.1080/02678299208029002.
[36] S.A. Rozanski, R. Stannarius, H. Groothues, F. Kremer, Dielectric properties of the nematic liquid crystal 4-fi-pentyl-4′-cyanobiphenyl in porous membranes, Liq. Cryst. 20 (1996) 59–66, https://doi.org/10.1080/02678299608032027.
[37] G.S. Attard, K. Araki, The study of director alignment in a nematogenic side-chain siloxane polymer by dielectric relaxation spectroscopy, Mol. Cryst. Liq. Cryst. 141 (1986) 69–75, https://doi.org/10.1080/00268948608080199.
[38] G.S. Attard, G. Williams, A.H. Fawcett, Dielectric relaxation spectroscopy studies on a polymer with mesogenic side chains, Polymer (Guildf.) 31 (1990) 928–934, https://doi.org/10.1016/0032-3861(90)90058-7.
[39] Y. Liu, Y. Li, H. Xiong, Dielectric chain dynamics of side-chain liquid crystalline polymer, ACS Macro Lett. 2 (2013) 45–48, https://doi.org/10.1021/mz3005988.
[40] M.H. Wolf, N. Izaguirre, B. Pascual-José, R. Teruel-Juanes, J. Labidi, A. Ribes-Greus, Dielectric characterisation of chitosan-based composite membranes containing fractionated kraft and organosolv lignin, React. Funct. Polym. (2023) 105833, https://doi.org/10.1016/j.reactfunctpolym.2024.105833.
[41] M.A. Khan, Z. Chen, New insights into the dynamics of poly(amidoamine) dendrimers with amino surface groups from segmental relaxation and ionic conductivity, Macromolecules 57 (2024) 6199–6208, https://doi.org/10.1021/acs.macromol.4c00774.